Very High Critical Field and Superior J_c-Field Performance in $NdFeAsO_{0.82}F_{0.18}$ with T_c of 51 K

By *Xiaolin Wang,* Shaban Reza Ghorbani, Germanas Peleckis,* and *Shixue Dou**

The discovery of the new family of oxypnictide superconductors,[1,2] including $LaFeAsO_{0.89}F_{0.11}$, with critical temperature T_c over 26 K, has brought new impetus to the fields of high-temperature superconductivity and strongly correlated electron systems. The new superconductors have the general formula REFeAsO, where RE is a rare earth element,[1–8] and show 2D crystal structures similar to those of high-T_c cuprate superconductors. They consist of alternating REO and FeAs layers, providing charge carriers and conducting planes, respectively. T_c is strongly dependent on the sizes of the rare earth element ions,[1–8] as well as on F-doping on oxygen sites[1,2] and oxygen deficiency in F-free material.[4] The upper critical field, H_{c2}, has been estimated to be higher than 55 or 63–65 T in $LaFeAsO_{0.9}F_{0.1}$,[6,7] 70 T in $PrFeAsO_{0.85}F_{0.15}$, and over 100 T in $SmFeAsO_{0.85}F_{0.15}$.[7] The two gap superconductivity proposed for $LaFeAsO_{0.9}F_{0.1}$ suggests that the H_{c2} could be further increased[6] to a significant extent. This is one of the unique features of the FeAs-based new superconductors. In this work, we show that $H_{c2}(48\,K) = 13$ T, and that the $H_{c2}(0)$ values can exceed 80–230 T in a high-pressure (HP) fabricated $NdO_{0.82}F_{0.18}FeAs$ bulk sample with T_c of 51 K. We also demonstrate that the supercurrent density in fields from 1 up to 9 T only drops by a factor of 2–6 for $T < 30$ K, significantly slower than for MgB_2 and high-T_c cuprate superconductors. The very high H_{c2} of the sample greatly surpasses those of MgB_2 and classic low-temperature superconductors, and the superior J_c-field performance is promising for the use of the new $NdFeAsO_{0.82}F_{0.18}$ superconductors in high-field applications.

The X-ray diffraction (XRD) and refinement results shown in Figure 1 indicate that the $NdFeAsO_{0.82}F_{0.18}$ sample is nearly single phase, with a tetragonal structure of the $P4/nmm$ symmetry and lattice parameters $a = 3.953$ Å and $c = 8.527$ Å. The Nd and As are located at the Wyckoff position 2*c*, with $z = 0.143$ and 0.659, respectively. The nearest neighbor distances are d(Nd–O) = 2.321 Å, d(Fe–As) = 2.397 Å, d(La–As) = 3.268 Å, and d(Fe–Fe) = 2.795 Å. These lattice parameters and bond lengths are smaller than those of $LaFeAsO_{0.89}F_{0.11}$, due to the fact that the size of the Nd^{3+} ion is smaller than that of the La^{3+}. A small amount of Nd_2O_3 (less than 1.7 wt%) is present as the second phase.

The temperature dependence of the resistivity of the $NdFeAsO_{0.82}F_{0.18}$ is shown in Figure 2. The resistivity is about 9 mΩ · cm at 300 K and 3 mΩ · cm at 52 K, while the residual resistivity ratio is $RRR = \rho(300\,K)/\rho(52\,K) = 3$, which means that the scattering becomes large at the onset temperature. The resistance drops to zero at $T = 46$ K in zero magnetic field. It can be seen that the onset T_c drops very slowly with increasing magnetic field. However, the $T_c(0)$ decreases quickly to lower temperatures. The upper critical field, H_{c2}, is defined as the field at which the resistance starts to drop. We use a criterion of 99% of normal resistivity at the onset temperature. The H_{c2} defined in this way refers to the case of a field parallel to the *ab*-plane, H_{C2}^{ab}.

The magnetoresistance $R(B)$ was also measured at several temperatures, as shown in Figure 3. The broad $R(B)$ transition is similar to what has been seen in a $LaFeAsO_{0.82}F_{0.18}$ sample.[6] Using the same analysis used in Ref. [6], the maximum (B_{max}), midpoint transition (B_{mid}), and minimum (B_{min}) fields are defined as 90, 50, and 10% of the normal state resistance $R_n(T_c)$, respectively. The magnetoresistance plots enabled us to extract some high-field data by extrapolation of $R(B)$ at $B < 13$ T to $R(B) = 0.9\ R_n(T_c)$, $0.5\ R_n(T_c)$, and $0.1\ R_n(T_c)$, as shown by the dashed lines in Figure 3. We can also define B_{max} (90% R_n), B_{mid} (50% R_n), and B_{min} (10% R_n) from the R–T curves. The magnetic-loop measurements indicate that the magnetization loops are almost reversible at $T > 20$ K and $B < 8.7$ T. This clearly implies that the $B_{max}(T)$ and B_{min}(T) from both the R–T and $B(H)$ curves can be regarded as the temperature dependences of

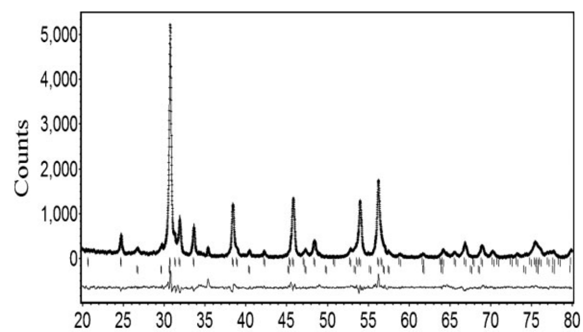

Figure 1. The observed (crosses), calculated (solid line), and difference diffraction (bottom solid line) profiles at 300 K for $NdFeAsO_{0.82}F_{0.18}$. The top peak markers relate to NdFeAsO, while the lower peak markers relate to the impurity Nd_2O_3. The peak at 35 degrees is characteristic of boron nitride.

[*] Prof. X. L. Wang, Prof. S. X. Dou, Prof. S. R. Ghorbani, Dr. G. Peleckis
Institute for Superconducting and Electronic Materials
University of Wollongong
Wollongong, NSW 2522 (Australia)
E-mail: xiaolin@uow.edu.au; shi@uow.edu.au
Prof. S. R. Ghorbani
Department of Physics, Tarbiat Moallem University of Sabzevar
P.O. Box 397, Sabzevar (Iran)

DOI: 10.1002/adma.200801527

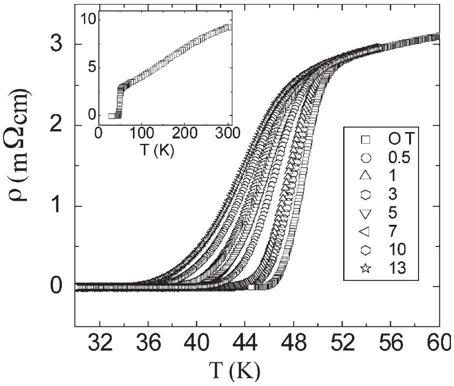

Figure 2. The temperature dependence of the resistivity of $NdFeAsO_{0.82}F_{0.18}$, measured in fields up to 13 T. The inset shows the ρ–T curve from 5 to 300 K.

$H_{c2}{}^{ab}$and $H_{c2}{}^{c}$. All these defined fields are plotted in Figure 4 as a comparison.

The slope of $H_{c2}{}^{ab}$ near T_c (99% R_n from the R–T curves), that is, $dH_{c2}{}^{ab}/dT$, is -5.8 T K^{-1}. This value, obtained from our $NdFeAsO_{0.82}F_{0.18}$ sample, is larger than that for $LaFeAsO_{0.89}F_{0.11}$ ($dH_{c2}/dT \approx 2$ T K^{-1}) and $SmFeAsO_{0.85}F_{0.15}$ ($dH_{c2}/dT \approx 5$ T K^{-1}).[5] The estimated slopes $dH_{c2}{}^{ab}/dT$ for H_{max} (90% R_n) and $dH_{c2}{}^{c}/dT$ for H_{min} (10% R_n) are 5.6 and 2.5 T K^{-1}, respectively.

Below B_{min}, a low measurement current density of 0.07 A cm^{-2} can flow through the sample via a percolative path. The $H_{c2}{}^{ab}(0)$ can be estimated using the Werthamer–Helfand– Hohenberg (WHH) formula: $H_{c2}{}^{ab}(0) = -0.69T_c(dH_{c2}^{ab}/dT)_{T=Tc} = 204$ T for the field at 99% R_n and 195 T for 90% R_n. $H_{c2}{}^{c}(0) = -0.69T_c(dH_{c2}^{c}/dT)_{T=Tc} = 80$ T. Using the Ginzburg–Landau (GL) equation:

$$H_{c2}(T) = H_{c2}(0)\frac{1-t^2}{1+t^2} \quad (1)$$

where $t = T/T_c$ is the reduced temperature and $H_{c2}(0)$ is the upper critical field at temperature zero. Figure 4c shows the fit of the GL theory to the experimental data for the high-temperature range. $H_{c2}{}^{ab}(0)$, $H_{c2}{}^{ab}$(midpoint), $H_{c2}{}^{ab}$(90%), and $H_{c2}{}^{ab}$(99%) are estimated to be 80, 150, 230, and 310 T, respectively. It should be pointed out that although the WHH and GL equations may not be valid for the low-temperature range, the H_{c2} values estimated using both equations are usually far below the real experimental data. According to Ref. [6], the real $H_{c2}{}^{ab}$values are at least 3–6 times higher than those estimated using the WHH equation, as seen in $LaFeAsO_{0.9}F_{0.1}$.[6] These indicate that the real H_{c2} in the $NdFeAsO_{0.82}F_{0.18}$ sample should be higher than what we estimated from the WHH and GL equations. Furthermore, a strong paramagnetic state was observed, and became dominant in high magnetic fields below T_c, as seen in a $NdFeAsO_{0.89}F_{0.11}$ sample.[9] This renders it difficult to estimate the H_{c2} from the magnetization measurements. Therefore, we believe that the determination of H_{c2} using the transport method, as shown in this work, is more convenient and reliable compared to magnetization measurements.

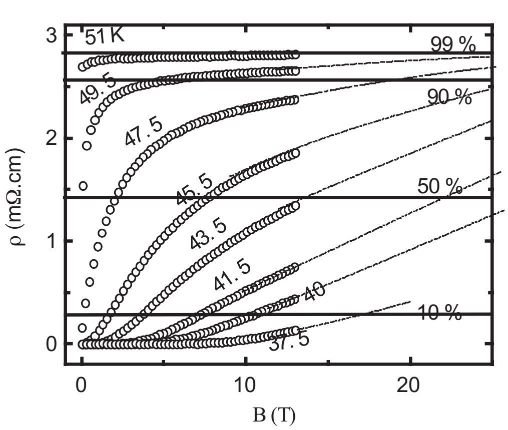

Figure 3. The resistivity $\rho(B)$ for different temperatures, taken in swept fields in a 14 T magnet with a measurement current of 1 mA.

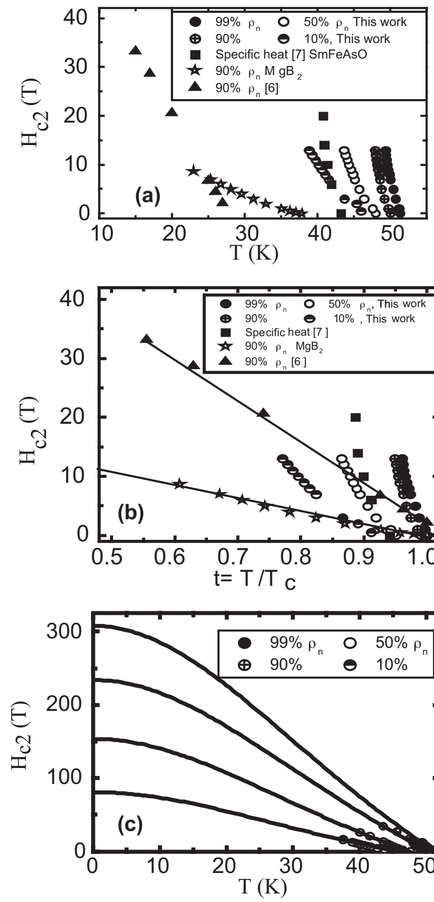

Figure 4. a,c) Field–temperature and b) field–reduced temperature plots derived from measurements of the resistivity against temperature and against the magnetic field. H_{c2} is variously defined as the field at which the resistivity drops 99, 90, 50, and 10% from its normal state near T_c. The data determined by a 90% drop in resistance for MgB_2 and LaFeAsO, and by heat capacity measurements for SmFeAsO, are also given. The solid lines in c) show the theoretical values based on GL theory (Eq. 1). The solid lines in b) are only guides to the eyes.

According to our data, the estimated anisotropy for $NdFeAsO_{0.82}F_{0.18}$ is $\Gamma = (H_{c2}{}^{ab}/H_{c2}{}^{c})^2 = 15$ and 8.3 for $H_{c2}{}^{ab}$ (99%) and $H_{c2}{}^{ab}$ (90%), respectively, in good agreement with what has been predicted from the resistivity ratio, $\Gamma = \rho_c/\rho_{ab}$ of 10–15 for LaFeAsO.[10]

The GL formula for the coherence length (ξ) is $\xi = (\Phi_0/2\pi\mu_0 H_{c2})^{1/2}$, where $\Phi_0 = 2.07 \times 10^{-7}$ Oe cm^2. This yields a zero temperature coherence length ξ of 10.3 Å for H_{c2} at 99% R_n, 14.5 Å for H_{c2} at 50% R_n, and 12 Å for H_{c2} at 90% R_n. These values are significantly smaller than those reported for $LaFeAsO_{0.89}F_{0.11}$ (35 Å),[10] and comparable to those of high-temperature superconducting cuprates.

As a comparison, $H_{c2}{}^{ab}$ and $H_{c2}{}^{c}$ for MgB_2 ($T_c = 39$ K), $LaFeAsO_{0.89}F_{0.11}$ ($T_c = 27$ K), and $SmFeAsO_{0.89}F_{0.11}$ ($T_c = 45$ K) are also plotted as a function of real and reduced temperatures (T/T_c), as shown in Figure 4a and b. Noticeably, the $NdFeAsO_{0.82}F_{0.18}$ sample shows the largest slopes and highest values of both $H_{c2}{}^{ab}$ and $H_{c2}{}^{c}$.

The typical ferromagnetic loops, which have been seen for $T < T_c$ and $T > T_c$ in Sm-based FeAs samples,[7] are absent in $NdFeAsO_{0.82}F_{0.18}$. This result rules out the presence of ferromagnetic impurities, such as Fe or Fe_2O_3. The magnetization loops show a strong paramagnetic background, believed to be contributed to by the paramagnetic state of Nd^{3+}.[10] According to magneto-optical imaging studies, the intragrain critical current density is about 6×10^4 A cm^{-2} at 20 K at low field for the $NdFeAsO_{0.82}F_{0.18}$ prepared using the HP method. We calculated J_c for our samples on the basis of $J_c = 20\Delta M/a(1 - a/3b)$, where ΔM is the height of the magnetization loop and a and b are the dimensions of the sample perpendicular to the magnetic field, $a < b$, using the size of the whole sample and the average size of grains, assuming that the current flows only within grains. ($J_c = 3\Delta M/\langle R\rangle$, where $\langle R\rangle$ is the average grain size.) The J_c field dependence is shown in Figure 5. It can be seen that J_c based on the sample size is above 10^4 A cm^{-2}, which is lower than what should exist in individual grains. However, the value of J_c based on the individual grains (assuming that the average grain size is about 50–100 μm[12]) is about $2 \times 10^5 - 1 \times 10^6$ A cm^{-2} at 5 K, in agreement with the result obtained from the magneto-optical imaging method ($J_c \approx 2.8 \times 10^5$ A cm^{-2}). It should be noted that J_c has a very weak dependence on field and remains constant for $B > 2$ T and $T = 5$ K. However, the value drops by less than one and two orders of magnitude for high fields of 8 T at 5 K and 20–30 K, respectively. Furthermore, for $B > 1$ T, J_c decreases only by a factor of 2–6, for $T < 30$ K. These results indicate that the $NdO_{0.82}F_{0.18}FeAs$ exhibits a superior J_c–field performance compared to MgB_2, whose J_c drops very quickly at 20 and 30 K, even at low fields.

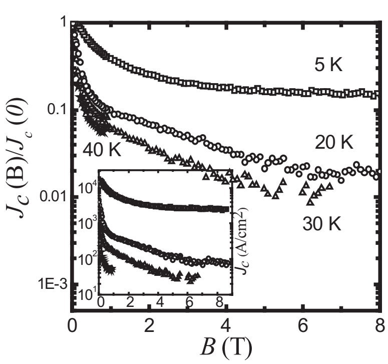

Figure 5. Normalized J_c versus field at different temperatures. The inset shows J_c calculated from magnetic measurements based on the real sample size.

In summary, we have shown that the superconductor $NdFeAsO_{0.82}F_{0.18}$, fabricated using a HP technique, exhibits a weak J_c–field dependence. The upper critical field values of H_{c2}(48 K) = 13 T and H_{c2}(0) can exceed 80–230 T, similar to high-T_c cuprate superconductors and surpassing the values of all low-temperature superconductors and of MgB_2. Such a high H_{c2} value and weak J_c–field dependence render NdFeAsO superconductors powerful competitors, which will be potentially useful in very high field applications. The H_{c2} value of these materials has the potential to be enhanced even further, through proper chemical doping (other rare-earth doping) and through physical approaches, due to the two-gap superconductivity in the new FeAs-based superconductor. The challenge now is to produce these materials with improved texture and connectivity, in order to allow these new superconductors to carry a high-enough critical current density.

Experimental

A polycrystalline sample with the nominal composition $NdFeAsO_{0.82}F_{0.18}$ was prepared using a HP technique. Powders of NdAs, As, Fe, Fe_2O_3, and FeF_2 were well mixed, pelletized, and then sealed in a boron nitride crucible and sintered at 1250 °C for 2 h under high pressure (6 GPa).[3] The phases in the sample were investigated by powder XRD, and the structure was refined using Rietveld refinement. Standard four-probe resistivity measurements were carried out on a bar sample using a physical-properties measurement system (PPMS, Quantum Design) in the field range from 0 to 13 T. Magnetic loops were also collected at various temperatures below T_c. The critical current density was calculated using the Bean approximation.

Acknowledgements

The authors thank the Australian Research Council for funding support through Discovery projects DP0558753 and DP0770205. We would like to thank Profs. Z. A. Ren and Z. X. Zhao from the Institute of Physics, Chinese Academy of Sciences for providing the sample used in this work.

Received: June 3, 2008
Revised: August 8, 2008
Published online: October 30, 2008

[1] Y. Kamihara, T. Watanabe, M. Hirano, H. Hosono, *J. Am. Chem. Soc.* **2008**, *130*, 3296.
[2] X. H. Chen, T. Wu, G. Wu, R. H. Liu, H. Chen, D. F. Fang, *Nature* **2008**, *453*, 761.
[3] Z.-A. Ren, J. Yang, W. Lu, W. Yi, G.-C. Che, X.-L. Dong, L.-L. Sun, Z.-X. Zhao, *Europhys. Lett.* **2008**, *82*, 57002.
[4] J. Yang, Z.-C. Li, W. Lu, W. Yi, X.-L. Shen, Z.-A. Ren, G.-C. Che, X.-L. Dong, L.-L. Sun, F. Zhou, Z.-X. Zhao, *Supercond. Sci. Technol.* **2008**, *21*, 082001.
[5] Z.-A. Ren, W. Lu, J. Yang, W. Yi, X.-L. Shen, Z.-C. Li, G.-C. Che, X.-L. Dong, L.-L. Sun, F. Zhou, Z.-X. Zhao, *Chin. Phys. Lett.* **2008**, *25*, 2215.

[6] F. Hunte, J. Jaroszynski, A. Gurevich, D. C. Larbalestier, R. Jin, A. S. Sefat, M. A. McGuire, B. C. Sales, D. K. Christen, D. Mandrus, *Nature* **2008**, *453*, 903.
[7] C. Senatore, R. Flükiger, G. Wu, R. H. Liu, X. H. Chen, *Cond-mat*, arXiv: 0805.2389, to be published in *Phys. Rev. B*.
[8] W. Lu, X.-L. Shen, J. Yang, Z.-C. Li, W. Yi, Z.-A. Ren, X.-L. Dong, G.-C. Che, L.-L. Sun, F. Zhou, Z.-X. Zhao, *Cond-mat*, arXiv:0804.3725.
[9] C. Tarantini, A. Gurevich, D. C. Larbalestier, Z. A. Ren, X. L. Dong, W. Lu, Z. X. Zhao, *Cond-mat*, arXiv:0805.4445v.
[10] D. J. Singh, M. H. Du, *Phys. Rev. Lett.* **2008**, *100*, 237003.
[11] A. S. Sefat, M. A. McGuire, B. C. Sales, R. Jin, J. Y. Howe, D. Mandrus, *Phys. Rev. B* **2008**, *77*, 174503.
[12] R. Prozorov, M. E. Tillman, E. D. Mun, P. C. Canfield, *Cond-mat*, arXiv:0805.2783.